OFFICE BUILDINGS WITH ELECTROCHROMIC WINDOWS: A SENSITIVITY ANALYSIS OF DESIGN PARAMETERS ON ENERGY PERFORMANCE, AND THERMAL AND VISUAL COMFORT

Jean-Michel Dussault, Louis Gosselin*

Department of Mechanical Engineering, Université Laval, Quebec City, Quebec, Canada, G1V 0A6

Article accepté pour publication dans : Energy and Buildings, Volume 153, 15 October 2017.

Abstract

In this paper, a representative office building zone with an electrochromic (EC) glazed façade was simulated in TRNSYS and Radiance/Daysim for a large number of different combinations of design parameters (i.e. location, façade orientation, window control, window-to-wall ratio, internal gains, thermal mass and envelope air tightness). Results of energy consumption, peak energy demand, useful daylight index (UDI) and predicted percentage of persons dissatisfied (PPD) for a total of 7680 scenarios were obtained and used in a sensitivity analysis considering the Main effect of the building parameters. The relative influence of the parameters is presented and the different designs improving the outputs are determined. Results have shown that the greatest total energy savings considering EC windows are for warmer climates with higher solar radiation exposures. The presence of an EC window mostly influences the cooling peak load and acts as an alternative solution to thermal mass from the perspective of peak reductions. While the choice of the specific window control strategy is having a limited impact on the energy savings and peak load reductions, the analysis revealed that this parameter has a larger impact on the visual comfort (UDI). The use of smart window does not appear to greatly influence the thermal comfort within the zone (small impact on the PPD).

Keywords: smart windows; electrochromic windows; rule-based control; building energy efficiency; thermal and visual comfort; sensitivity analysis; main effect; design parameters

* Corresponding Author: Louis.Gosselin@gmc.ulaval.ca; Tel.:+1-418-656-7829; Fax: +1-418-656-5343.

Nomenclature

ACH	Air change per hour, 1/hr
C	Volume heat capacity, kJ/m^{3}K
CDD	Annual cooling degree days considering a 18°C reference temperature, °C-day
CDT	Cooling design temperature, °C
CE	Cooling energy consumption reduction (or increase), kWh/m^2
CPED	Cooling peak energy demand reduction (or increase), W/m^2
D	Depth, m
Dz	Daylight zone
E	Energy consumption, kWh/m^2
E_z	Zone air distribution effectiveness
EC	Electrochromic
f	Fraction
H	Height, m
HDD	Annual heating degree days considering a 18°C reference temperature, °C-day
HDT	Heating design temperature, °C
HE	Heating energy consumption reduction (or increase), kWh/m^2
HPED	Heating peak energy demand reduction (or increase), W/m^2
I	Incident solar radiation, W/m^2
I75	Infiltration rate (rated at 75Pa gage pressure), L/s-m^2
IG	Internal gains, W/m^2
IGDB	International Glazing Database
LDD	Luminaire Dirt Depreciation
LED	Artificial lighting system with LEDs
LLD	Lumen Lamp Depreciation
LPD	Light Power Density, W/m^2
ME	Main effect
N	Number of parameters considered for sensitivity analysis
n	Number of possible designs for a parameter
Ori	Orientation
PPD	Predicted Percentage of Dissatisfied, %
R_a	Outdoor air flow rate required per unit area, L/s-pers
R_p	Outdoor air flow rate required per person, L/s-pers
RBC	Rule-based control

σ	Standard deviation
S	Number of possible design
SHGC	Solar heat gain coefficient
SW	Smart window
T	Temperature, °C
TE	Total energy consumption reduction (or increase), kWh/m^2
TM	Thermal mass
TPED	Total peak energy demand reduction (or increase), W/m^2
Tsol	Solar transmittance, %
Tvis	Visible transmittance, %
UDI	Useful daylight illuminance, %
W	Width, m
Wp	Workplane
WWR	Window to wall ratio
X	Set of building parameters (model inputs)
x	Building parameter
Y	Model outputs
y	Output for a specific set of building parameters **X**

Subscripts

1%	Annual cumulative frequency of occurrence exceeding the given dry bulb temperature
99%	Annual cumulative frequency of occurrence exceeding the given dry bulb temperature
ave	Average
cool	Cooling
heat	Heating
k	k^{th} building parameter
L	Light output
LW	Wall section of the building façade below the glazing
min	Minimum
max	Maximum
n	Number of possible designs for parameter k
nat	Natural light illuminance
out	Exterior conditions
P	Light power input

req	Requirement
sp	Setpoint
sum	Summer conditions
tot	Total
UW	Wall section of the building façade above the glazing
v	Vertical
w	Window
win	Winter conditions
z	Zone

1 Introduction

Smart windows (SW) are window technologies offering a control flexibility in terms of solar heat gains, daylight and glare in building perimeter zones. This flexibility is achieved through their capacity to adapt their optical properties (ranging from a clear state to a fully colored state) through different type of stimuli such as gas concentration, temperature, solar radiation or an applied voltage. Among the most promising SW technologies, electrochromic (EC) windows (whose tinted states are controlled by an applied voltage) provide views to the outside regardless of their colored states, limit glare [1] and are seen as the most reliable and promising technologies in the field of energy-efficient window technologies [2].

Although current EC window technologies are offering a great range of properties [2] [3] [4] [5], the use such technologies also requires a good understanding of the appropriate control to be implemented as well as an established communication network with other relevant systems (such as with the artificial lighting or HVAC systems) [6]. With the increasing interest toward EC technologies in the last decades, outcomes from numerical and field studies on the topic were published and has led to the diffusion of early-market design guidance information [7].

Early numerical simulations of office buildings compared a spectrally selective low-E window technology with EC technologies (reflective and idealized) in a cooling dominated location [8]. Three control strategies were considered, i.e. control based on daylight, on solar radiation or on space load. Results revealed that the total energy savings could be achieved by using EC windows compared to the conventional low-E windows and that the daylight control was offering the best overall energy performance. Similar simulation results were also obtained in other studies considering other locations [9], residential applications [10] or heating dominated climates [11].

A field study [12] analyzed the performance of electrochromic windows controlled in various ways so as to optimize daylight while avoiding glare compared to a spectrally selective low-e window. This study monitored lighting energy reduction of 26% ± 15% and a cooling load reduction of 7 ± 4%.

A recent study on advanced control strategies [13] for smart windows also has shown that heuristic controls give quite good energy and comfort performance compared to quasi optimal controllers based on genetic algorithms and model predictive control. Heuristic controls thus seem to be so far the best trade-off control strategies in terms of ease of implementation versus potential benefits (energy and comfort wise).

Nowadays, the advances in the field of EC windows have led to new field studies combining EC technologies with other complementary technologies such as photovoltaic cells [14] or ventilated façades [15].

Despite evidence that smart windows can enhance building performance in specific scenarios, there is still a lack of general and systematic design guidelines to introduce smart windows in building designs. In particular, it is difficult to establish which building designs are the most improved by using smart windows, and to what extent. Sensitivity analysis techniques have recently been gaining a lot of attention in order to identify the most influential design variables in terms of building performance [16]. For example, a recent study has presented an uncertainty and sensitivity analysis of energy and visual performances for an office building with external venetian blind shading in a hot-dry climate [17]. It was found that glazing design parameters such as the window-to-wall ratio (WWR), the glazing type, the blind orientation and the slat angle were the most influential. Another study combined sensitivity analysis and simulation-based optimization in order to optimize the thermal and energy performance of residential buildings in the Argentine littoral region [18]. The case under study has proven that this approach could drastically improve the thermal and energy performance. These examples highlight the fact that sensitivity analysis techniques emerge as a useful tool for building design process, but not precedent was found in which they were used for building designs with smart windows.

The main objective of this study is to provide decision-making information on building design with efficiently controlled electrochromic windows. In this paper, a sensitivity analysis is presented to assess the relative effect of the main building design parameters on energy and comfort improvements related with the use of a smart window. Section 2 introduces the building energy and daylight models and the sensitivity analysis technique that was developed for the present work. A series of simulations in which several building design variables were varied simultaneously was performed. Based on the concept of "Main effect", the most significant variables influencing energy consumption, peak demand and comfort in the presence of SW are reported in Section 3.

2 Methodology

2.1 Simulation software

In this study, energy and comfort performance data were obtained for office buildings using TRNSYS, a state-of-the-art and flexible transient system simulation tool [19]. The TRNSYS built-in multi-zone building model (Type 56) offers the possibility to adapt the window properties at every simulation time step through a variable window ID feature. This feature

facilitates the assessment and comparison of different smart window control strategies. While the building thermal model (section 2.3), the thermal comfort model (section 2.4) and the control strategies (section 2.6) were directly implemented within TRNSYS, the daylight and artificial light simulations (section 2.5) were performed with Daysim [20] and Radiance [21], respectively, and inputted into TRNSYS in the form of lookup tables. Batch files for parametric study and the post-processing of results were implemented within MATLAB. A simulation time step of one hour was used in this work.

2.2 Climates

Simulation results were obtained for ten US and Canadian locations (see Table 1) selected to cover a wide range of climates. EnergyPlus weather data files (.epw files) were used for simulations. Table 1 presents annual heating and/or cooling features for each location, i.e. heating degree days (HDD), cooling degree days (CDD) and averaged end-use energy consumption (total (E_{tot}), heating (E_{heat}) and cooling (E_{cool})) as well as their respective standard deviations (σ). Only the energy required for heating, cooling and lighting was included in the total energy consumption. Energy and standard deviation results in Table 1 are presented per unit of floor area. HDD values were calculated from the same weather data files that were used for simulations. Averaged values for E_{tot}, E_{heat} and E_{cool} and their standard deviations were obtained over a series of building designs for a given location (city) as explained later. Note that the values of E_{tot} in Table 1 might appear to be small compared to typical total energy intensity of the current Canadian and American building stocks, but it should be mentioned that it only includes the sensible energy required for the heating, cooling and lighting of a high-performance modern building. In this study, latent loads were not considered since SWs only affect sensible loads.

Table 1 - Climate information

Locations	HDD [°C-day]	CDD [°C-day]	E_{tot} [kWh/m^2]	$\sigma_{E,tot}$	E_{heat} [kWh/m^2]	$\sigma_{E,heat}$	E_{cool} [kWh/m^2]	$\sigma_{E,cool}$
US locations (ASHRAE 90.1 zones)								
Atlanta, GA (3A)	1673	896	34.3	10.5	1.5	1.9	23	8.8
Chicago, IL (5A)	3429	506	35.2	6.7	9.0	7.4	16	6.7
Miami, FL (1A)	68	2442	43.5	12.8	0.0	0.0	34	10.0
New-Orleans, LA (2A)	707	1597	37.7	11.8	0.3	0.4	28	9.3
San Francisco, CA (3C)	1557	22	28.5	12.0	0.1	0.3	19	9.5
Washington, D.C. (4A)	2293	880	32.6	8.6	3.0	3.5	20	7.9
Canadian locations (ASHRAE 90.1 zones)								
Calgary, AB (7)	5147	40	37.0	7.3	13.2	9.7	13.6	7.4
Montreal, QC (6A)	4493	234	37.5	7.6	12.5	9.6	14.9	6.9
Toronto, ON (6A)	4089	232	35.6	7.1	11.8	9.4	13.5	6.1
Vancouver, BC (5A)	3020	5	28.0	7.3	3.6	4.0	13.9	7.0

2.3 Building model

2.3.1 Building geometry and construction

A representative six-sided box-shaped office zone of the building was modeled with 100 m^2 of floor area, i.e. 10 m width (W) by 10 m depth (D), and a ceiling height of 3 m (H). The plenum zone was not modeled. Four different orientations (north, east, south and west) were simulated for the exterior façade wall. The façade is composed of an electrochromic smart window (see Section 2.6 for further details on the smart window system and properties) and an opaque exterior wall (concrete siding, lightweight frame filled with mineral wool insulation and gypsum indoor finishing) with a U-value of 0.45 W/m^{2}K. All other surface boundary conditions of the model (internal walls, floor and ceiling) were modeled considering identical zone conditions for adjacent zones. In this study, direct solar gains were assumed to be uniformly distributed on the floor (geosurf = 1). On the other hand, diffuse solar gains were distributed according to absorption-transmission weighted area ratios for all surfaces (TRNSYS simple model).

Three different window-to-wall ratios (WWR = 0.33, 0.50 and 0.67) were considered in the study. For every façade configuration, the window width corresponded to the zone width (10 m) and the window sill was located at 1 m above the floor.

Two building façade air tightness ratings (rated at 75 Pa [22]) were considered in this study, i.e. a modern air tight construction (0.5 ACH) and a leakier envelope construction (2

ACH). Hourly infiltration rates were calculated in the model based on the façade rating adjusted with weather data such as outside air temperature (T_{out}) and wind speed [23].

The concrete floor slab thicknesses was varied between two values, i.e.: 0.038 m (1.5 inch) and 0.254 m (10 inches) (i.e. C=71.53 kJ/m^{2}K and 476.86 kJ/m^{2}K, respectively). These two floor constructions were selected to represent different values of the effective thermal mass of the zone (low versus high).

2.3.2 Gains and schedules

Internal gains account for artificial lighting, occupancy and equipment. Based on the purpose of this work, only sensible heat has been included in the model. Two scenarios were studied for internal gains, i.e. low internal gains and high internal gains [24]. Table 2 presents the building zone heat gains as well as their respective radiative and convective fractions for the low and high internal gain scenarios, respectively.

Table 2 - Low and High internal gains (net sensible)

	Radiative [W]		**Convective [W]**		**Total [W]**		**Total/floor area [W/m2]**	
	Low	**High**	**Low**	**High**	**Low**	**High**	**Low**	**High**
Equipment	350	1050	150	450	500	1500	5	15
Lighting	188	375	130	261	318	636	3	6
Occupants (5)	263	525	113	225	375	750	4	8
Total	800	1950	393	936	1193	2886	12	29

To represent a typical transient variation of internal gains and lighting requirements in office buildings, week schedules have been created based on the ASHRAE 90.1 (Table G-I) schedules for office occupancy. The only internal gains considered during week-ends were the electronic appliances at 15% of their maximal power usage.

2.3.3 Lighting system

Two types of artificial lighting systems were considered for the study. The first type of lighting system relies on sixteen T8 lamps (64 W of nominal power per lamp) (lamp dimensions of 0.54 m width × 1.15 m long) uniformly distributed over the ceiling. Based on the technological advances in the field of artificial lighting [25], a second high-efficiency lighting system has also been simulated. For simplicity, this system presents the same lamp dimensions and position as for the first lighting system; however the T8 lamps are replaced by

a more efficient LED system consuming half the power of the T8 lamps for the same illuminance output (32 W of nominal power per LED lamp). While the T8 lamps lighting system is part of the high internal gains scenario presented in the previous subsection (High gains in Table 2), the LED lighting system is considered in the low internal gains scenario (Low gains in Table 2). Artificial lighting system properties are summarized in Table 3. The daylight zone dimming control presented in Table 3 is based on the workplane illuminance setpoint (Wp_{sp}). The required artificial light output fraction (f_L) is calculated to respect Wp_{sp}. The light power input fraction is then obtained based on the value of f_L. Figure 1 illustrates the artificial lighting system layout.

Table 3 - Artificial lighting systems

Nominal LPD	10.2 W/m^2 (T8 lamps) and 4.4 W/m^2 (LED system)
Ballast factor (T8 lamps)	0.86
GDF	0.81 (GDF = LDD · LLD = 0.9 ·0.9)
Wp_{sp}	500 lux (on the sensor "S" in Figure 1) during occupancy
Daylight zone dimming control	$f_P = \begin{cases} 0 & f_L = 0 \\ f_{P,min} & 0 < f_L < f_{L,min} \\ \left[f_L + (1 - f_L) f_{P,min} - f_{L,min} \right] / (1 - f_{L,min}) & f_{L,min} \le f_L \le 1 \end{cases}$

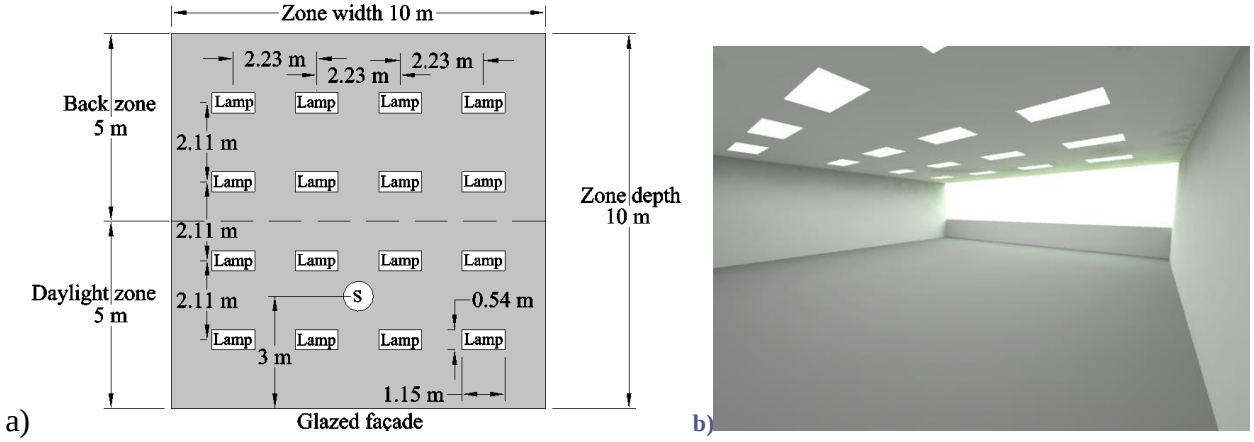

Figure 1: (a) Artificial lighting system disposition (Top view), (b) 3D representation of the zone natural and artificial light sources simulated with Daysim and Radiance, respectively.

2.3.4 HVAC system

It was assumed that the calculated heating load Q_{heat} and cooling load Q_{cool} acted directly on the air node of the building model, and were satisfied instantly by the HVAC&R system. The cooling system considers a constant coefficient of performance (COP) of 3. The indoor temperature was allowed to vary between 21°C and 25°C during occupancy, based on the acceptable ranges of temperatures provided in ASHRAE 55-2013. Outside of the occupancy hours, these temperature limits are respectively lowered and raised by 3°C. The heating and cooling systems were sized to meet the heating/cooling requirements at all time. The required flow rate of outside air was calculated based on the ASHRAE 62.1-2016 standard with the breathing zone outdoor airflow calculations considering an outdoor airflow rate per person of 2.5 L/s-pers, an outdoor airflow rate per unit area of 0.3 L/s-m^2 and a zone air distribution effectiveness (E_z) of 0.8. A heat exchanger was used to recover heat between the air exhaust and make up air with 60 % efficiency. Note that all the heating and cooling energy needs reported in this paper are the energy consumed to satisfy the thermal loads and not the thermal loads themselves.

2.4 Thermal comfort model

The thermal comfort was assessed through the calculation of the Predicted Percentage of Dissatisfied (PPD) as defined in the 7730 ISO Standard [26]. Occupants' conditions (clothing, metabolic rate and relative air velocity) for typical winter and summer seasons were defined based on ASHRAE 55 requirements and are summarized in Table 4. The only difference between winter and summer conditions is the clothing number since people's clothing is influenced by the surrounding conditions [27]. In this work, values of PPD were calculated at each time step for both the winter (PPD_{win}) and summer clothing conditions (PPD_{sum}). The actual PPD indicator at each time step was then chosen between PPD_{win} and PPD_{sum} based on the corresponding daily averaged PPD offering the smallest percentage of dissatisfaction. This approach captures the occupants' decisions to adapt their clothing based on the surrounding conditions.

Table 4 - Winter and summer conditions fort thermal comfort

	Winter conditions	**Summer conditions**
Clothing factor [clo]	1.0	0.5
Metabolic rate [met]	1.1	1.1
Relative air velocity [m/s]	0.1	0.1

The calculation of the PPD also involves the zone air temperature and the mean radiant temperature (T_{MR}), which are both calculated through the TRNSYS model internal calculations. This model assumes that T_{MR} is the area weighted mean surface temperature of all surfaces of the zone. Although this model would only give a rough approximation of the actual T_{MR} within a specific zone, this approach is widely used in practical engineering applications [28] and gives results accurate enough to evaluate the level of thermal comfort within the zone.

2.5 Lighting monitoring and visual comfort model

To offer proper lighting on the workplane (at a 0.8 m height from the floor level) in terms of minimal illuminance requirements, a light sensor has been positioned at the center of the room width and at a 3 m depth from the glazed wall (represented by the "S" symbol in Figure 1). Illuminance measurements on this sensor are defined as the representative values for the workplane of the daylight zone (Dz). The luminosity requirement (WP_{req}) on the sensor has been set to 500 lux [29] during occupancy hours. For both lighting system types (T8 and LED), the lamps were controlled in two separate groups (i.e. the lamps of the daylight zone and the lamps of the back zone). While the back zone lamps were fully switched on at all time during occupancy hours, the lamps of the daylight zone were dimmed in a fashion similar to the EnergyPlus Continuous/OFF dimming control [30] to assure minimal visual comfort requirements while taking advantage of daylight whenever possible (see Table 3 for further details regarding the daylight zone dimming control). The index used to assess the visual comfort (through useful daylight levels) in the building zone is the Useful Daylight Illuminance (UDI). In this work, the UDI is defined as the percentage of hours of the working year where daylight illuminance values on the workplane fall between 100 lx and 2000 lx, inclusively. The higher the UDI, the more likely it is that occupants feel comfortable from the visual standpoint.

While daylight is desired in building zones to improve occupant's visual comfort, natural light could also cause visual discomfort such as glare in situations of overabundance. Many indicators have been developed in the past to assess the glare potential in perimeter buildings zones [31]. In this paper, the glare potential was assessed with a maximal illuminance setpoint of 2000 lx [32]. Situations where illuminance values were over 2000 lx on more than 20% of the workplane in the daylight zone area were considered as periods of visual discomfort caused by glare.

2.6 Window system and control strategies

The smart window modeled in this study has a 1.63 W/m^{2}K U-value. The double glazing includes an electrochromic layer whose optical properties can be varied by an applied voltage [2]. The electrochromic layer was applied on the surface 2, i.e. the internal surface of the external glazing, in order to limit undesired solar heat gains from absorbed and reemitted heat as well as to increase thermal and visual comforts. Four possible states of opacity, from clear to dark, have been included in the model. Table 5 provides the SW center of glazing Solar Heat Gain Coefficient (SHGC), visible transmittance (Tvis) and solar transmittance (Tsol) properties at normal incidence. While properties at normal incidence of Table 5 are presented for readers' benefits, one should note that the model uses the complete and detailed angle dependent properties available in the IGDB (International Glazing Database available online) and obtained through the use of Berkeley Lab WINDOW software.

Table 5 - Smart window center-of-glazing properties

Smart window states	**SHGC [-]**	**Tvis [%]**	**Tsol [%]**
State 1 (S1) (bleached)	0.47	62.1	38.1
State 2 (S2)	0.17	21.2	8.6
State 3 (S3)	0.11	5.9	2.4
State 4 (S4) (fully tinted)	0.09	1.5	1.0

In the model, every time the state of the window is changed, the corresponding properties of that new state are also applied to the window. Since the time step (one hour) considered in the simulation results is greater than the time required to switch from one state to the other (about 5 minutes considering an ideal window designed with a sufficient amount of bus bars) [33], it was assumed that window properties over a time step were constant.

In this paper, three main types of rule-based control (RBC) strategies were considered (i.e. RBC based on daylight [12] [34], vertical solar radiation (incident on the zone façade) [34] [35] and net window heat flux [36]) and are explained in the following subsections. Table 6 presents the main parameters considered in each RBC strategy. As illustrated in Table 6, every RBC considers glare control as defined in Section 2.5. Each type of RBC also considers either two or four possible states for control, i.e.: a 2 state (clear/dark) control and 4 state (clear/dark + 2 intermediary states) control.

Table 6 - Smart window rule-based control (RBC) strategies

RBC ID	RBC type	RBC setpoints	Glare control	Possible SW states
RBC1	Daylight	$Wp_{nat,max}$ = 500 lx	$ill_{max,Dz}$ = 2000 lx	2 states
RBC2				4 states
RBC3	I_v	$I_{v,max}$ = 95 W/m^2	$ill_{max,Dz}$ = 2000 lx	2 states
RBC4		$I_{v,max}$ = 315 W/m^2		4 states
RBC5		$I_{v,min}$ = 63 W/m^2 $I_{v,max}$ = 95 W/m^2		2 states
RBC6		$I_{v,min}$ = 63 W/m^2 $I_{v,max}$ = 315 W/m^2		4 states
RBC7	q_{net}	T_{ave} = 23°C	$ill_{max,Dz}$ = 2000 lx	2 states
RBC8				4 states

In this paper, the use of a controlled smart window refers to a smart window considering a control logic based on one of the RBCs presented in Table 6.

Daylight (RBC1 and RBC2)

In these cases, the SW state decisions were based on a three level control scheme as illustrated in Figure 2. First of all, the controller evaluates if the building zone is in cooling mode or not. For occupancy hours where the building is in cooling mode, a control trade-off appears between the undesired solar heat gains and the desired natural light. In such situations, the control is based on the selected RBC strategy. The RBC strategies aim at selecting a SW state allowing some natural light to enter into the zone (to increase daylight and reduce lighting energy) while trying to limit overheating (to reduce cooling loads) and glare. Outside occupancy hours, the trade-off disappears and the controller selects the colored SW state, S4, to limit cooling loads as much as possible. On the other hand, when the building is not in cooling mode, the SW controller is set to maximize daylight/solar heat gains. In such situations, while the bleached SW state, S1, is selected during non-occupancy hours, the clearest state that respects glare requirements (see Section 2.5) is selected during occupancy hours.

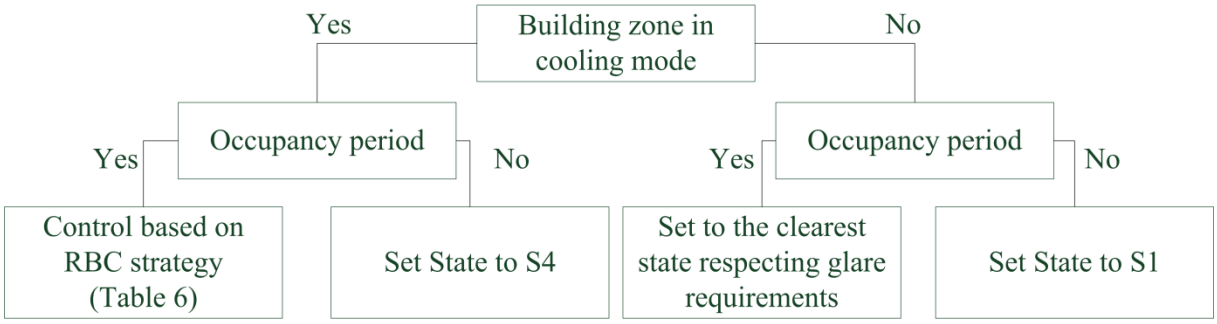

Figure 2: Daylight and I_v RBC schemes

The daylight control strategies (i.e. RBC1 and RBC2 in Table 6) monitor the daylight illuminance on the workplane (sensor "S" Figure 1) and select the SW state that maximizes it without over lighting ($Wp_{nat,max}$ = 500 lx) to limit heat gains within the zone. One should note that glare control has priority over daylight control (i.e., if glare occurs in a situation where daylight on the workplane is not maximized, the SW state will still change to a darker state that meets glare control requirements). The daylight controls strategies work identically for both the 2 state and 4 state controls.

Iv – incident vertical solar radiation (RBC3 to RBC6)

The SW state decisions were based on the three level control scheme illustrated in Figure 2. However, in this case, the RBC (i.e. RBC3 to RBC6 in Table 6) is based on the vertical solar radiation (I_v) incident on the zone façade. The SW state is selected based on setpoints for I_v. For the 2 state control, only one setpoint ($I_{v,max}$) is defined. If I_v is greater than $I_{v,max}$, the SW state is switched to the colored state S4. Otherwise ($I_v \leq I_{v,max}$), the SW state is set to the bleached state S1. For the 4 state control, two setpoints ($I_{v,min}$ = 63 W/m^2 and $I_{v,max}$) were defined. While bleached state is selected when $I_v \leq I_{v,min}$, the colored state is selected when $I_v > I_{v,max}$. The two intermediate state are chosen (linear interpolation) when I_v falls between the two threshold setpoints. In this work, two values for $I_{v,max}$ were studied (i.e., $I_{v,max}$ = 95 W/m^2 and $I_{v,max}$ = 315 W/m^2) [8]. As for the daylight control, glare control has priority over the control on I_v for this type of RBC.

RBC based on incident solar radiation are seen are very promising heuristic control strategies due to their relatively simple control scheme and potentially inexpensive solar radiation sensors [37].

Net window heat flow control (RBC7 and RBC8)

This type of RBC bases its decisions according to the net heat flow, q_{net}, passing through the window:

$$q_{net} = U_w \cdot (T_{out} - T_z) + SHGC \cdot I \quad (1)$$

where U_w is the overall window heat transfer coefficient, T_{out} and T_z are the exterior and interior air temperatures, SHGC is the overall window solar heat gain coefficient and I is the total incident solar radiation.

In the net heat flow control [36], the state of the SW is selected based on q_{net}, the zone temperature (T_z) and the average temperature value between the minimum and maximum zone temperature setpoints ($T_{ave} = (T_{z,min} + T_{z,max})/2$). If $T_z \leq T_{ave}$, the space is considered to be in heating mode (closer to heating) and the state offering the higher q_{net} will be selected. On the other hand, for $T_z > T_{ave}$, the space is considered to be in cooling mode and the SW state offering the lowest q_{net} will be selected.

While the heat transfer coefficient (U_w) of some dynamic window technologies such as blinds within the glazing could be influenced by the state of the window [36], the heat transfer coefficient of the EC window considered in this work remains the same regardless of the window color state. This being said, one could state that the net heat flow as defined in Eq. 1 will thus always be larger for state S1 compared to state S2, and for state S2 compared to state S3 and so on. The net heat flow control algorithm as described above thus simplifies as follows. For the 2 state control, the bleached state S1 is selected for $T_z \leq T_{ave}$ and the colored state S4 is selected for $T_z > T_{ave}$. For the 4 state control, the bleached state S1 is selected for $T_z \leq T_{z,min}$, S2 is selected for $T_{z,min} < T_z \leq T_{ave}$, S3 is selected for $T_{ave} < T_z \leq T_{z,max}$, and the colored state S4 is selected for $T_z > T_{z,max}$. Similarly to the daylight and solar radiation RBC control types, the glare control for this type of RBC has priority over the net heat flow control decisions.

2.7 Sensitivity analysis – Main effect

In this paper, a sensitivity analysis was performed to assess the effect of the principal design parameters (**X**) on different outputs (**Y)** for buildings with smart windows. Table 7 presents the eight building parameters (N = 8) under study. These parameters were selected based on the fact that they are common design parameters and/or relevant parameters related to smart windows. While other design parameters (such as the building envelope or other solar shading devices) could have been included in this study, the authors limited to eight the number of

parameters given the scope of this study and the extensive amount of simulations involved. While the 4th parameter (ID = 4) in Table 7 is considered in the analysis to assess the influence of replacing a reference window (represented by the passive clear state S1) by a controlled SW (with RBC), the 5th parameter can be used to compare the RBCs against each other. Each parameter (e.g., location, orientation, etc.) has been attributed an ID (k) and has a finite number (n_k) of possible values (e.g., the orientation is the second parameter (k = 2) with $n_k = n_2 = 4$ possible values, i.e. north, east, south and west). All possible combinations of the different parameters were simulated. Given the number of possible values for each parameter, a total of 7680 simulations were thus performed. Depending on the parameter under study, those 7680 simulation results are then organized into different subsets for the analysis.

Table 7 - Building design parameters studied in the sensitivity analysis

ID (k)	Parameter (X)	Possible values	Number of designs (n_k)	S_k
1	Location (City)	Atlanta | Chicago | Miami | New-Orleans | San Francisco | Washington | Calgary | Montreal | Toronto | Vancouver	10	768
2	Orientation (Ori)	North | East | South | West	4	1920
3	Window to wall ratio (WWR)	0.33 | 0.50 | 0.67	3	2560
4	Presence of a smart window (SW)	Yes | No	2	3840
5	SW rule-based controls (RBC)	RBC1 to RBC8	8	960
6	Internal gains (IG)	Low | High	2	3840
7	Thermal mass	Low | High	2	3840
8	Air tightness ratings at 75Pa (I75)	0.5 ACH | 2 ACH	2	3840

The analysis was based on the Main effect [38], i.e. a global sensitivity index that focuses on how the building parameters (**X**) influence the simulation outputs (**Y**). The Main effect of the kth parameter (x_k) on **Y** is denoted $ME_k(\mathbf{Y})$. To obtain $ME_k(\mathbf{Y})$, the 7680 simulations are separated according to the x_k values into n_k groups. In other words, all simulations with the same x_k values are gathered together. The average of the outputs **Y** in each group is then calculated:

$$\overline{Y}_{x_{kj}} = \frac{1}{S_k} \sum_{i=1}^{s_k} Y_{i,x_{kj}} \qquad 2$$

where $\sum_{i=1}^{S_k} Y_{i,x_{kj}}$ includes all the simulation results (i = 1, 2…, S_k) with the j^{th} possible value for x_k. Note that S_k is the number of sample in the group over which the outputs are averaged, i.e. $S_k = 7680/n_k$. The Main effect for this parameter x_k is then obtained by taking half the difference between the maximum and the minimum values of the n_k calculated $\overline{Y}_{x_{kj}}$:

$$ME_k(Y) = \frac{1}{2}\left(\overline{Y}_{x_k \max} - \overline{Y}_{x_k \min}\right) \quad 3$$

where

$$\overline{Y}_{x_k \min} = \min\left(\overline{Y}_{x_{kj}}\right)$$
$$\overline{Y}_{x_k \max} = \max\left(\overline{Y}_{x_{kj}}\right) \quad 4$$

Measured outputs (Y)

The outputs of interest for the sensitivity analysis, listed in Table 8, include energy consumption (total, heating, cooling and lighting), peak energy demand (total, heating and cooling) as well as visual and thermal comfort indices, i.e., UDI and PPD, respectively.

Table 8 - Measured output for sensitivity analysis

Outputs (Y)	**Units**
Energy improvements	
Total energy consumption (TE)	[kWh/m^2]
Heating energy consumption (HE)	[kWh/m^2]
Cooling energy consumption (CE)	[kWh/m^2]
Lighting energy consumption (LE)	[kWh/m^2]
Peak load improvements	
Total peak energy demand (TPED)	[W/m^2]
Heating peak energy demand (HPED)	[W/m^2]
Cooling peak energy demand (CPED)	[W/m^2]
Visual comfort improvements	
Useful Daylight index (UDI)	[%]
Thermal comfort improvements	
Predicted percentage of dissatisfied (PPD)	[%]

The goal of this paper being to assess the performance of SW regarding comfort and energy, every model output (obtained with smart window control) has been compared to a base case scenario considering exactly the same set of design parameters except for the controlled SW that is replaced by a conventional passive window (state S1 at all time). The output measurements used for the sensitivity analysis are thus improvements (or reductions, depending on the resulting signs). For example, if the total energy consumption improvement for a specific set of building parameters is reported as −10 kWh/m^2, one should understand that this specific configuration with a SW actually gives a 10 kWh/m^2 savings compared to the reference case with a passive window. Negative output values are beneficial in terms of energy, peak and PPD results (savings and thermal comfort improvements, respectively) but are detrimental for UDI (decrease of daylight availability). In this sense, the parameter ID 4 represents the improvements of the best SW control compared to the base case. One should note that the results of the outputs presented in this section are representative for perimeter zones of office buildings only.

The sensitivity analysis is divided into three subsections (Sections 3 to 3.3). Results are presented in a similar fashion for every subsection, i.e. ME results are presented first. Based on the ME results, further explanations are then given for the most influential parameters (relatively high values of ME). While the sign of the output measurements could be interpreted as improvements or deteriorations, as explained in the previous paragraph, one should keep in mind that the sign of ME results is always positive by definition (i.e. ME represents the spread between maximum and minimum averaged outputs). The ME could thus illustrate if a parameter has a lot of influence or not for a specific output; however it cannot explain alone how the variation of a parameter influences the outputs. Such explanations are obtained by the subsequent analysis guided by the ME results.

3 Results

Section 3.1 presents the results related to the energy use (total, heating, cooling and lighting). The total energy use is the summation of the heating, cooling and lighting energy. Section 3.2 presents the results related to the peak energy demand (total, heating and cooling). The total peak energy demand is defined as the peak load including heating, cooling and lighting. Finally, Section 3.3 presents the results related to visual and thermal comfort (i.e. UDI and PPD, respectively).

3.1 Main effects of building parameters on energy use reduction

Figure 3 illustrates the ME of the eight parameters on the different energy use outputs. As one would expect, the location (city), the façade orientation (ori) and the window to wall ratio (WWR) are among the most influential parameters (high ME values) regarding the total, heating and cooling energy use outputs (illustrated in Figure 3a, b and c). That being said, Figure 3 also shows that the presence of a well controlled smart window (SW) has as much influence as these other parameters on the total and cooling energy outputs, which highlights the relevance of considering with care the integration of smart windows during the design of a building. While the presence of a smart window (SW) has a great effect on the total energy output, the choice of the specific rule-based control strategy (RBC) also has an effect on the reduction of the total energy consumption, but it is relatively limited. This effect on total energy is mainly driven by the lighting energy (high value of ME_{RBC}(LE) as illustrated in Figure 3d). Figure 3d also illustrates that the artificial lighting energy is mostly affected by the parameters related to smart windows (SW and RBC) and the light system itself (LED versus T8 lamps considered in the internal gains (IG) parameters). On the other hand, the thermal mass and the building tightness present quite small effects (small ME results) on all types of energy use outputs, i.e. the energy benefit of using a SW is not influenced by thermal mass or air tightness. In Figure 3, one could observe that any parameter of influence for the total energy use (Figure 3a) is explained by one or more of its components (i.e. heating, cooling and lighting energy, Figure 3b, c and d, respectively). One should also note that the scale is greater for the cooling outputs (ME_k(CE)) compared to the heating and lighting outputs (ME_k(HE) and ME_k(LE), respectively). In other word, using a SW impacts mostly on the energy consumption for cooling.

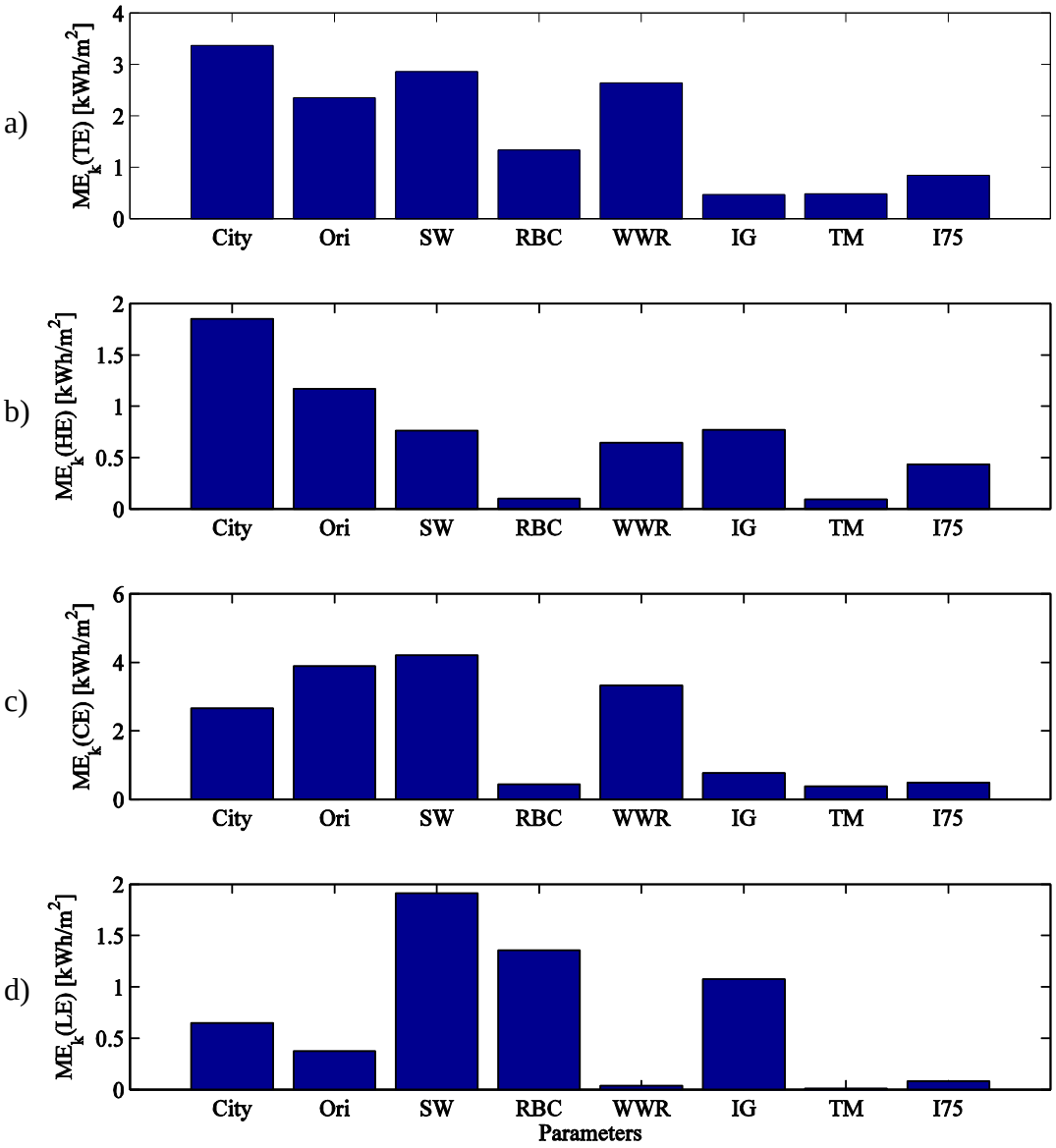

Figure 3: Main effect of parameters (model inputs) on change in energy consumption due to using a SW for a) total energy, b) heating, c) cooling and d) lighting.

Keeping in mind that the simulation results refer to the energy difference for buildings with SW compared to the same buildings with passive windows, a deeper analysis of the energy use outputs revealed that all the heating and lighting simulation results were positive values (i.e. increase of energy consumed due to using a SW) and that cooling results were all negative values (i.e. decrease in energy consumed due to using a SW). Since the base case scenarios consider the clear state of the SW at all time and because the use of SWs could only lead to equal or darker states compared to the base cases, it thus makes sense that equal or

lower values for heat gains and daylight are to be expected. These results reveal that the use of smart windows reduce cooling energy use, but also tend to increase the heating and lighting energy use (by limiting heat gains and daylight). These opposite trends resulted in 84.5% of the 7680 scenarios under study giving negative values of total energy use outputs (i.e. a reduction of the total energy consumption). While some situations where SWs were introduced (15.5 %) would lead to more energy being consumed, one should note that the integration of smart windows into building design generally leads to improvements in terms of total energy use. In this work, the building simulations resulting in the highest increase of total energy consumed were mostly occurring for building zones located in northern climates (such as Calgary, Montreal, Toronto and Chicago) with low internal gains and/or high infiltration rates. A particular attention should thus be paid during the design process to make sure that the design with SWs actually improves the overall energy performance. The following paragraphs provide additional indicators to support design decisions through the analysis of averaged total energy results.

Figure 4 presents the total energy savings for building zones with the smart windows averaged for each location as a function of their respective HDD (Figure 4a) and CDD (Figure 4b). The purpose of relating energy savings to HDD and/or CDD instead of the cities in Figure 4 is to extend the conclusions to a climate related parameter rather than specific cities. As illustrated in Figure 4, the reduction of the total energy use is larger for lower HDD (or for higher CDD) values. Said differently, the warmer the climate is, the higher the benefits are to use smart windows in terms of overall energy use. The relatively linear relations between the total energy savings and HDD or CDD are represented by the red line in Figure 4a and Figure 4b (although the linear relationship for CDD with energy consumption is less strong compared to HDD, the relation is still evident). The ME of the location of Figure 3a is explained through the difference between the extreme results illustrated in Figure 4 (i.e. difference between TE_{ave} for Miami and Toronto).

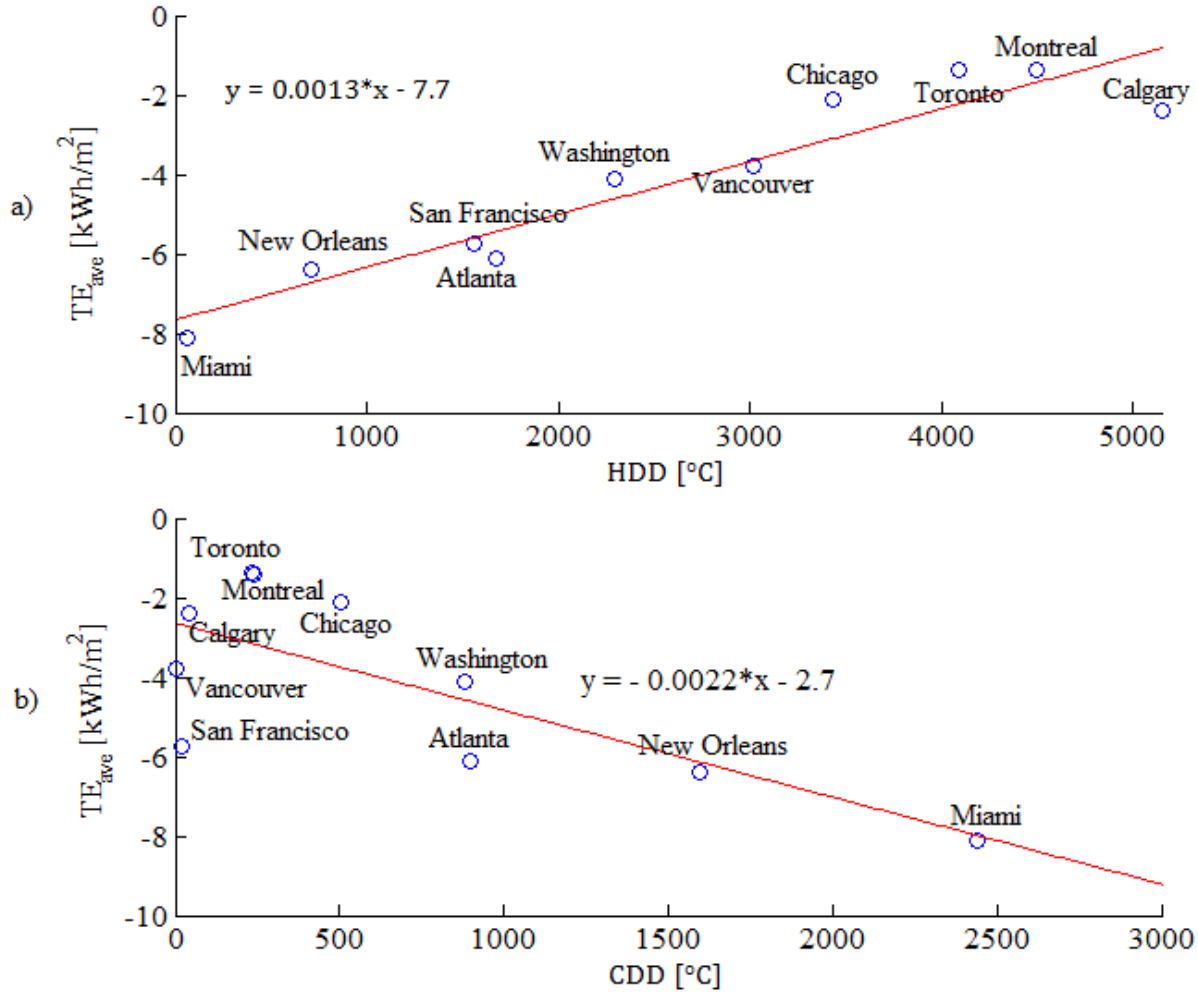

Figure 4: Total energy consumption reduction due to using a SW (averaged per city) as a function of the a) HDD and b) CDD

Figure 5 presents the averaged total energy savings for the four different façade orientations. As previously observed [39], Figure 5 shows that SW are offering larger benefits for east, south and west façades (savings of about 5 kWh/m^2) compared to the north façade (0.7 kWh/m^2 savings). The ME of the orientation in Figure 3a is explained in Figure 5 by the difference between the TE_{ave} for the north and the south façades.

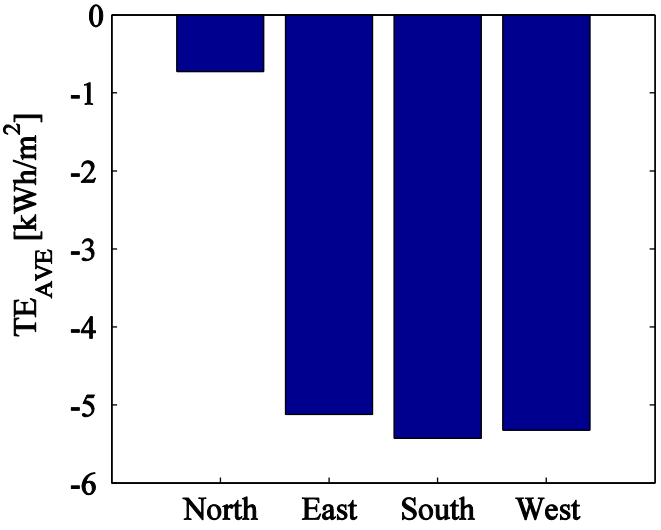

Figure 5: Total averaged energy use reduction due to using a SW for each orientation

Figure 6 presents the averaged total energy savings for the eight different smart window RBCs. Regardless of the control input (daylight, solar radiation or heat flow), the 2 state control strategies (RBC1, RBC3, RBC4 and RBC7) present lower total energy savings than their 4 state counterparts (i.e. RBC2, RBC5, RBC6 and RBC8). Overall, RBC2 and RBC6 (daylight with 4 states and I_v with 4 states with 63-315 W/m^2) give the greatest total energy savings with averaged savings on total energy use of 5.72 kWh/m^2 and 5.42 kWh/m^2, respectively. The integration of SW into office building design should thus consider at least 4 state controllers to benefit from the flexibility of the SW technology and should also integrate a control algorithm based on daylight or incident solar radiation. The ME of the RBC in Figure 3a is explained in Figure 6 by the difference between the TE_{ave} for RBC2 and RBC7.

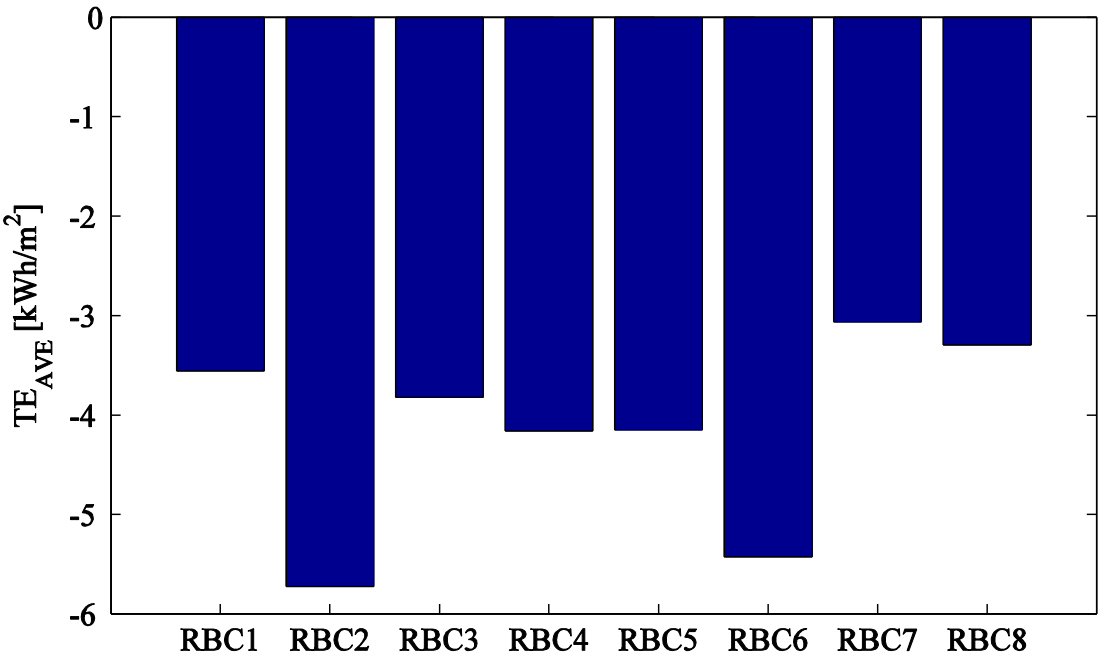

Figure 6: Total averaged energy use reduction due to using a SW for each RBC

Figure 7 presents the averaged total energy savings for the three different WWRs. As illustrated, the higher the WWR, the greater is the potential of total energy savings if controlled SWs are installed. However, even if this statement is true in general (or on average), one could anticipate based on the previous conclusions that some specific scenarios with high WWR would not lead to any savings (e.g. north building façades for colder climates). The ME of the WWR in Figure 3a is explained in Figure 7 through the difference between the TE_{ave} for WWR = 0.67 and WWR = 0.33.

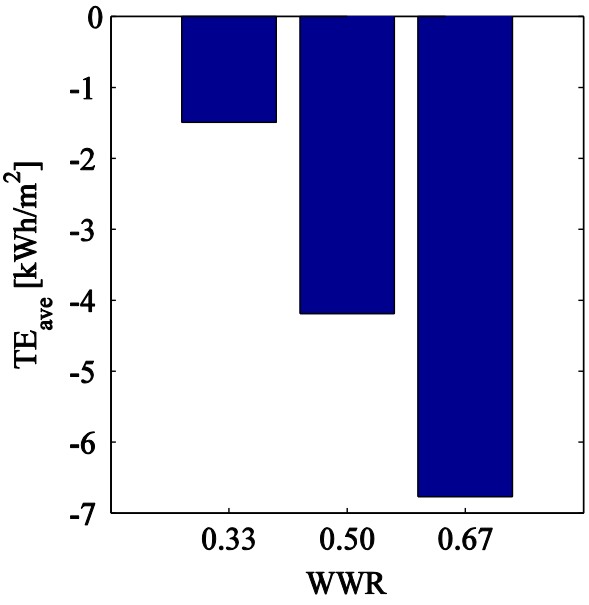

Figure 7: Total averaged energy reduction due to using a SW for each WWR

3.2 Main effect of building parameters on energy peak reduction

Figure 8 illustrates the ME of the eight parameters on the peak energy demand. While the location has the most influence on the total peak demand (Figure 8a), other parameters such as the façade orientation (Ori), the presence of a smart window (SW), the window to wall ratio (WWR) and the thermal mass (TM) also present a significant influence on the heating and cooling peak loads. As for the energy use outputs of the previous section (Section 3.1), the presence of a SW (control on the solar heat gains) has an influence on the heating and cooling peak loads (mostly cooling). On the other hand, the type of SW rule-based control (RBC) has a negligible impact on the heating and cooling peak loads.

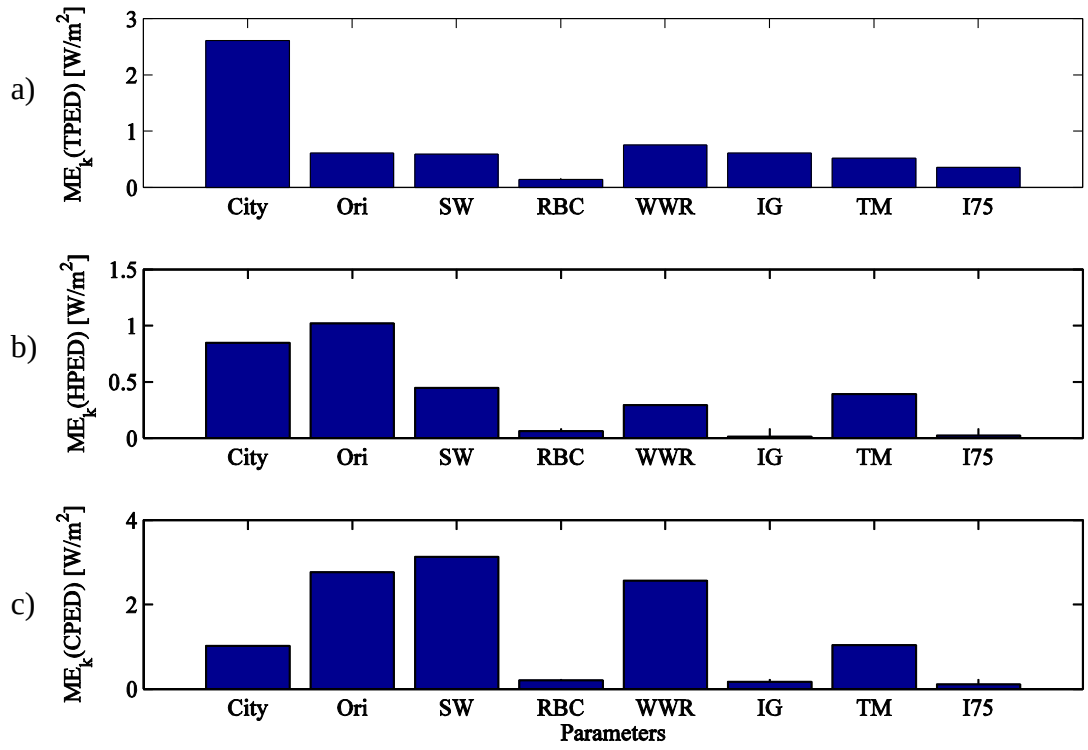

Figure 8: Main effect of the parameters (model inputs) on change in peak energy demand due to using SW for a) Total, b) Heating and c) Cooling)

As for the energy outputs, the reader should keep in mind that the peak energy demand outputs refer to the difference of peak demand between buildings using a SW and the same building designs with a passive window (passive state S1). Figure 9 presents the total averaged peak energy demand outputs for each location. In Figure 9, one could observe that the integration of a SW involves an increased total peak demand for some locations (positive

values) and a peak reduction for other locations (negative values). This behavior is mainly explained by the fact that the annual peaks could occur either during the heating or cooling period. Since controlled SWs can increase heating loads, but reduce cooling loads (as mentioned in Section 3.1), locations for which the annual peak occurs during a heating period see their total peak increase and locations having their peak during the cooling period see their total peak decrease. The spread between the results for Miami and Montreal in Figure 9 explains the ME_k(TPED) value of the location in Figure 8a.

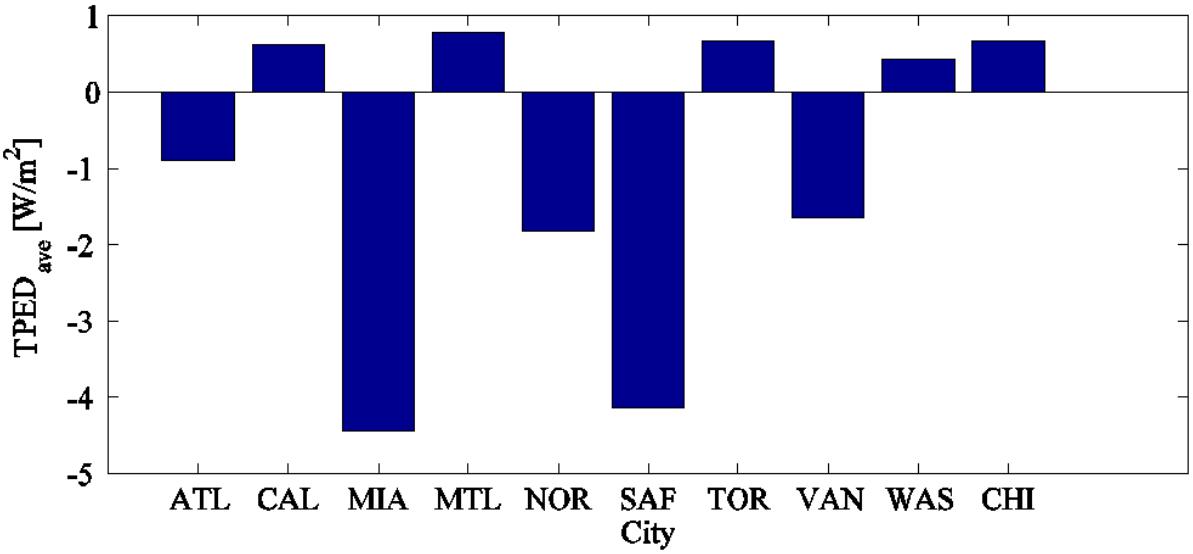

Figure 9: Total reduction (or increase) of averaged peak energy demand for each location

The individual assessment of the heating and cooling peaks gives valuable information for sizing these systems. From Figure 10a, one could note that the heating peak load is slightly increased for all cities (since SWs tend to limit solar heat gains). The integration of SW could thus likely force the heating system to be slightly larger compared to the base case scenario. However, Figure 10b revealed that cooling peak loads are reduced which means that the cooling system could be downsized accordingly compared to the base case scenario. All in all, the integration of SW into building design could thus potentially lead to net initial cost savings considering for the HVAC systems. However, further studies on the topic should be carried on to properly assess the impact of SW on HVAC systems costs.

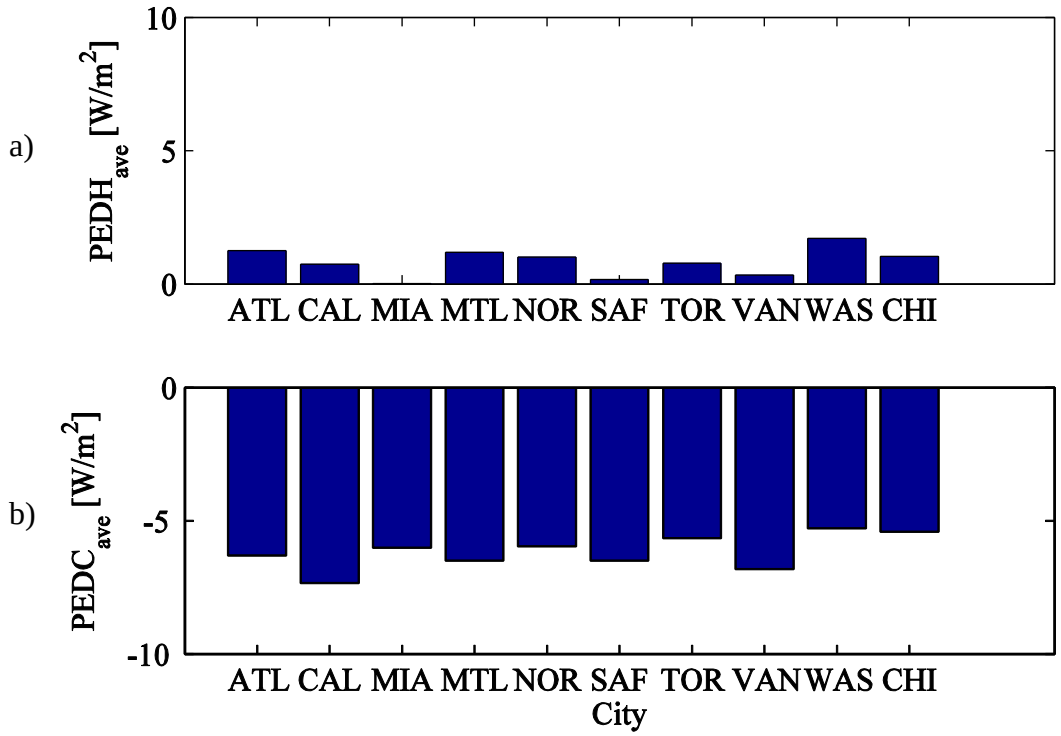

Figure 10: Averaged peak energy demand reduction (or increase) for each location (i.e. a) heating peak increase and b) cooling peak reduction)

The influence of the orientation, the SW control type and the WWR on total peak reduction presents a behavior very similar to the one of the total energy presented in the previous section. In terms of the orientation, the peak savings are greater for the east, south and west façades. As for the SW control type, the peak is more affected (higher savings) by the fact that a controlled SW is present (compared to the base case scenario) than by the difference between the different types of RBC (with RBC2 offering the best averaged total peak reduction, i.e. 1.18 W/m^2). Finally, the higher the WWR, the higher the peak reductions are when a controlled SW is considered.

Figure 11 presents the reduction of total averaged peak energy demand due to using a SW for the two values of thermal mass. Based on the results of Figure 11, one could realize that adding smart windows into building designs with lower thermal mass leads to greater peak reductions compared to designs with higher thermal mass. This behavior is explained by the fact that the thermal mass smooths out the cooling energy demand (time shifting of the radiative gains) even when no SW is used. This being said, including a SW properly controlled in a building design reduces the importance of having a high thermal mass to achieve a high level of performance regarding energy.

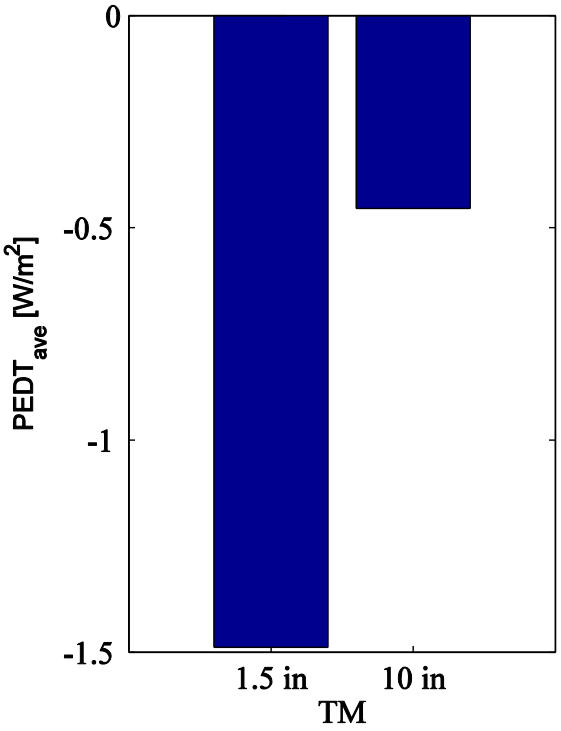

Figure 11: Averaged peak energy demand reduction for the two thermal mass designs

3.3 Main effects of building parameters on visual and thermal comfort improvements

Figure 12 illustrates the ME of the eight building parameters on the visual and thermal comfort. One could observe that the presence of a SW influences the visual and thermal comfort indicators (UDI and PPD), as illustrated in Figure 12a and b respectively. However, while the RBC has a low effect on the PPD (Figure 12b), it has the greatest influence on the UDI (Figure 12a). Considering absolute ME values, one could realize that the use of smart windows in building designs could largely influence the visual comfort (ME_k(UDI) up to 36.8% in Figure 12a). On the other end, even if some parameters (such as the location or the presence of a SW) are influencing thermal comfort, the ME_k(PPD) values only vary by up to 1.5%, thus revealing that SWs have a lot more influence on the visual comfort than on the thermal comfort. While the thermal model in this study was kept simple, further studies could focus on more detailed thermal comfort models to assess the impact of the use of SW on thermal comfort.

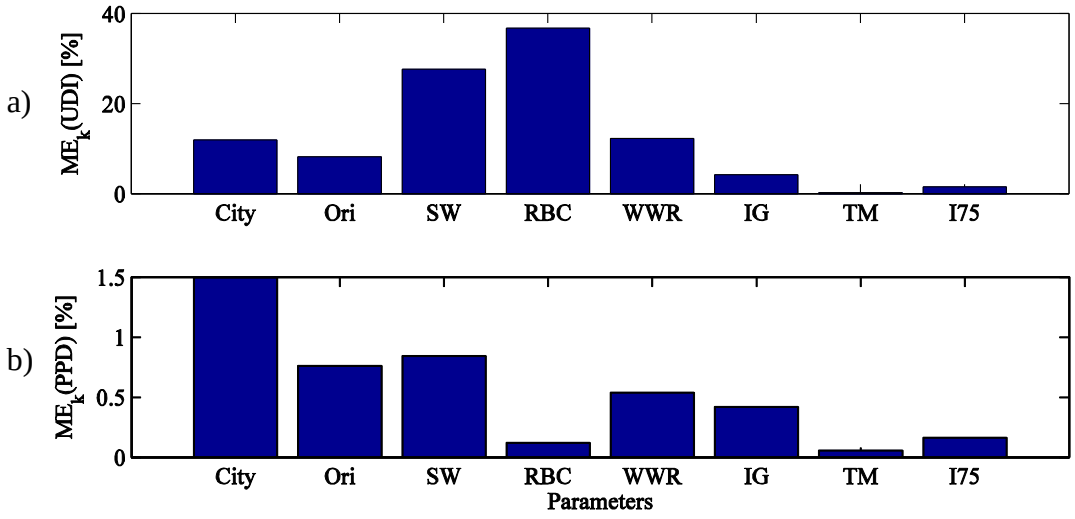

Figure 12: Main effect of the parameters on change in visual and thermal comfort due to using a SW (i.e. a) UDI and b) PPD, respectively)

Figure 13 presents the averaged UDI changes due to the SW for the eight RBCs. As illustrated, only two types of RBC actually improve the UDI on average, i.e. RBC2 and RBC6 that are both four state controllers with their control either based on daylight on the workplane and incident solar radiation, respectively. The analysis of the simulation results revealed that the RBC2 strategy leads to 89% of the scenarios improving the UDI compared to the base case (all other scenarios leading to the same values of UDI compared to the base case). In all cases for RBC2, scenarios leading limited UDI improvements or no UDI improvements at all were for north oriented façades and/or building façades with a low WWR (i.e. WWR = 33%). In such situations, a conventional passive window offers almost as much useful daylight on the workplane as a controlled SW would (with RBC2 control). However, in situations where the façade is facing east, south or west and for higher values of WWR, the daylight on the workplane exceeds more often the upper range limit of 2000 lx. In these situations, the use of a SW with RBC2 enables to maintain the daylight illuminance level on the workplane within the acceptable limits. The behavior for RBC6 is similar to RBC2, although performances are reduced. RBC6 strategy also leads to UDI deteriorations compared to the base case for north façades and the lowest WWR ratio. As mentioned previously, in order to keep the computational time and the length of the paper acceptable, results presented in this study are limited to building designs without overhangs. As presented in previous studies [40], overhangs combined with smart windows can further reduce glare. It is thus expected that ME results would have been reduced if the analysis was considering overhangs in the base case.

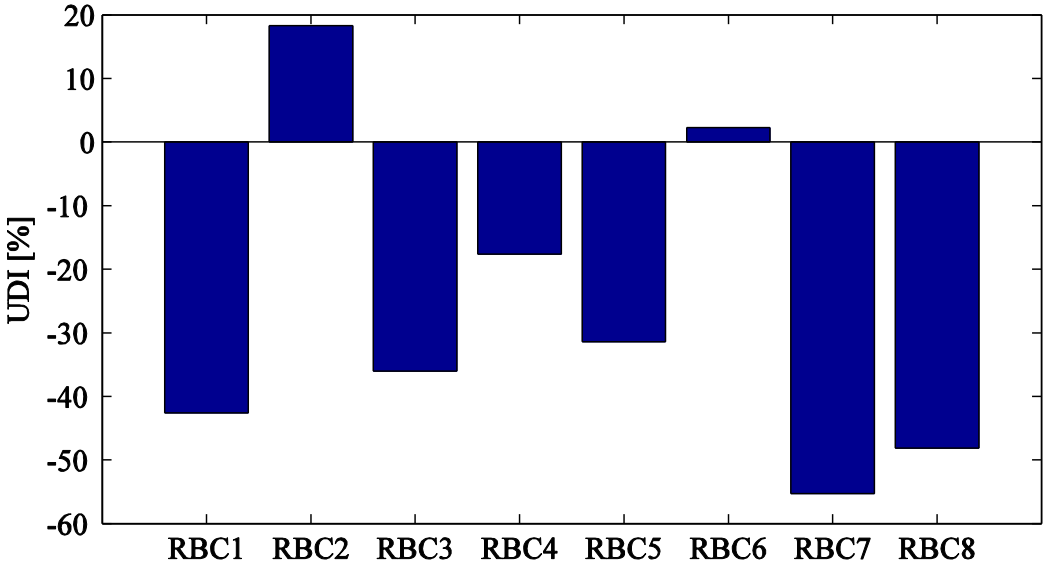

Figure 13: Averaged UDI reduction (or increase) for the eight RBC

4 Conclusions

This paper presents the sensitivity analysis of different design building parameters on energy and comfort indicators for buildings with electrochromic SWs. A representative office building zone was modeled considering an exterior glazed wall exposed to ambient conditions and all other surfaces (interior walls, ceiling and floor) exposed to adjacent zones with identical zone conditions.

The building parameters considered in the analysis were the location (10 different cities in Canada and in the U.S.), the façade orientation (north, east, south or west), the presence of a smart window and its applied control (8 different types of RBC), the WWR (33%, 50% or 75%), the internal gains density (low and high), the thermal mass (low and high) as well as the building air tightness (thigh and leaky envelopes). Simulations were performed for every combination of the aforementioned parameters, leading to a total of 7680 scenarios. Results for every scenario were compared to their respective reference case considering a passive window. Improvements or degradation of performance presented in this work are with respect to the reference scenarios.

The sensitivity analysis was performed considering the ME of the building parameters on the energy consumption savings (total, heating, cooling and lighting), the peak energy demand reductions (total, heating, and cooling), the increase of useful daylight index (UDI) and the reduction of predicted percentage of dissatisfied (PDD). The ME was used to target the most influential parameters.

It was shown that the presence of SWs has quite a considerable influence on the energy consumption results (mainly on the total, cooling and lighting energy consumptions). The SW actually has as much influence on the change of total and cooling energy consumptions as the location, the façade orientation or the WWR. While SWs tend to slightly increase heating and lighting energy consumption by limiting solar gains and daylight, they provide considerable cooling savings. These behaviors resulted in total energy savings for approximately 85% of the scenarios under study, with the remaining 15% of the scenarios leading to energy consumption deteriorations (occurring for south facing building zones located in northern climates with low internal gains and/or high infiltration rates). The greatest total energy savings considering SWs are to be expected for warmer climates, for east, south or west façades and for high WWR values. While the different RBCs have very little impact on the heating and cooling, they influence the total energy consumption through the lighting loads. The RBC strategies RBC2 and RBC6 were found to be the most performant in terms of energy savings.

The analysis of the ME results on the peak energy demands revealed that the presence of a smart window mostly influences the cooling peak loads and that the choice of the RBC strategy has very little impact on the peak reduction. Due to the fact that SWs limit solar gains and that the annual peak load could occur either during the heating or cooling season, the integration of SW involves an increased annual total peak demand for colder climates and an annual peak reduction for warmer climates. In all cases, the use of a SW leads to increased heating and reduced cooling peak loads (compared to the reference scenarios). It was also shown that adding smart windows into building designs with lower thermal mass leads on average to greater peak reductions compared to designs with higher thermal mass.

While the choice of the RBC is having a limited impact on the energy savings and an even lower impact on the peak loads, the ME analysis revealed that this parameter has a very large impact on the UDI. Only two RBC strategies, i.e. RBC2 and RBC6, were found to offer visual comfort improvements (on average) compared to the reference scenarios with passive windows (with RBC2 outperforming RBC6). As for thermal comfort, the results showed that the use of smart windows has a limited effect on PPD.

The results presented in this work aim at helping the decision-making related to electrochromic SWs in the building design process. While total energy savings, peak load reductions and visual/thermal comfort indicators were assessed in this paper, further studies using a similar approach should include additional relevant decision making information regarding SW. Among other, future studies should include the relative effect of overhang

designs [41], active load management window strategies [42], integrated control strategies [43] and should consider the economic challenges related to the integration of smart windows. The Main effect of the building variables on the total cost (initial and operational) could also be studied.

While this work focused on the decision-making related to electrochromic SWs in the building design process, the methodology developed in this work could be applied to alternative technologies such as dynamically controlled shading systems. Further studies could focus a comparison of such technologies.

Acknowledgments

Dussault's and Gosselin's work was supported by the Natural Sciences and Engineering Research Council of Canada (NSERC).

References

[1] R. D. Clear, V. Inkarojrit, and E. S. Lee, "Subject responses to electrochromic windows," *Energy Build.*, vol. 38, no. 7, pp. 758–779, Jul. 2006.

[2] B. P. Jelle, A. Hynd, A. Gustavsen, D. Arasteh, H. Goudey, and R. Hart, "Fenestration of today and tomorrow: A state-of-the-art review and future research opportunities," *Sol. Energy Mater. Sol. Cells*, vol. 96, no. 1, pp. 1–28, Jan. 2012.

[3] R. Baetens, B. P. Jelle, and A. Gustavsen, "Properties, requirements and possibilities of smart windows for dynamic daylight and solar energy control in buildings: A state-of-the-art review," *Sol. Energy Mater. Sol. Cells*, vol. 94, no. 2, pp. 87–105, 2010.

[4] S. V. Vasilyeva, P. M. Beaujuge, S. Wang, J. E. Babiarz, V. W. Ballarotto, and J. R. Reynolds, "Material Strategies for Black-to-Transmissive Window-Type Polymer Electrochromic Devices," *ACS Appl. Mater. Interfaces*, vol. 3, no. 4, pp. 1022–1032, Apr. 2011.

[5] A. Piccolo and F. Simone, "Performance requirements for electrochromic smart window," *J. Build. Eng.*, vol. 3, pp. 94–103, Sep. 2015.

[6] E. S. Lee, D. L. DiBartolomeo, F. M. Rubinstein, and S. E. Selkowitz, "Low-cost networking for dynamic window systems," *Energy Build.*, vol. 36, no. 6, pp. 503–513, 2004.

[7] E. Lee, "A Design Guide for Early-Market Electrochromic Windows," Lawrence Berkeley National Laboratory, LBNL-59950, 2006.

[8] R. Sullivan, E. S. Lee, K. Papamichael, M. Rubin, and S. E. Selkowitz, "Effect of switching control strategies on the energy performance of electrochromic windows," presented at the Proc. SPIE 2255, Optical Materials Technology for Energy Efficiency and Solar Energy Conversion XIII, Germany, 1994, vol. 2255, pp. 443–455.

[9] R. Sullivan, M. D. Rubin, and S. E. Selkowitz, "Energy performance analysis of prototype electrochromic windows," *ASHRAE Trans.*, vol. 103, no. pt 2, pp. 149–156, 1997.

[10] R. Sullivan, M. Rubin, and S. Selkowitz, "Reducing Residential Cooling Requirements Through the Use of Electrochromic Windows," in *Thermal Performance of the Exterior Envelopes of Buildings VI Conference*, Clearwater, Florida, 1995.

[11] R. Sullivan, E. Lee, M. Rubin, and S. Selkowitz, "The Energy Performance of Electrochromic Windows in Heating-Dominated Geographic Locations," presented at

the SPIE International Symposium on Optical Materials Technology for Energy Efficiency and Solar Energy Conversion XV, Freiburg, Germany, 1996.
[12] E. S. Lee, D. L. DiBartolomeo, and S. E. Selkowitz, “Daylighting control performance of a thin-film ceramic electrochromic window: Field study results,” *Energy Build.*, vol. 38, no. 1, pp. 30–44, Jan. 2006.
[13] J.-M. Dussault, M. Sourbron, and L. Gosselin, “Reduced energy consumption and enhanced comfort with smart windows: Comparison between quasi-optimal, predictive and rule-based control strategies,” *Energy Build.*, vol. 127, pp. 680–691, Sep. 2016.
[14] A. L. Dyer, R. H. Bulloch, Y. Zhou, B. Kippelen, J. R. Reynolds, and F. Zhang, “A Vertically Integrated Solar-Powered Electrochromic Window for Energy Efficient Buildings,” *Adv. Mater.*, vol. 26, no. 28, pp. 4895–4900, Jul. 2014.
[15] M. Pittaluga, “The electrochromic wall,” *Energy Build.*, vol. 66, pp. 49–56, Nov. 2013.
[16] M. H. Kristensen and S. Petersen, “Choosing the appropriate sensitivity analysis method for building energy model-based investigations,” *Energy Build.*, vol. 130, pp. 166–176, Oct. 2016.
[17] R. Singh, I. J. Lazarus, and V. V. N. Kishore, “Uncertainty and sensitivity analyses of energy and visual performances of office building with external venetian blind shading in hot-dry climate,” *Appl. Energy*, vol. 184, pp. 155–170, Dec. 2016.
[18] F. Bre, A. S. Silva, E. Ghisi, and V. D. Fachinotti, “Residential building design optimisation using sensitivity analysis and genetic algorithm,” *Energy Build.*, vol. 133, pp. 853–866, Dec. 2016.
[19] R. C. G. M. Loonen, F. Favoino, J. L. M. Hensen, and M. Overend, “Review of current status, requirements and opportunities for building performance simulation of adaptive facades,” *J. Build. Perform. Simul.*, vol. 0, no. 0, pp. 1–19, Mar. 2016.
[20] C. Reinhart and P.-F. Breton, “Experimental validation of 3ds Max® design 2009 and Daysim 3.0,” in *11th International IBPSA Conference - Building Simulation 2009, BS 2009, July 27, 2007 - July 30, 2007*, Glasgow, Scotland, 2009, pp. 1514–1521.
[21] G. J. Ward, “The RADIANCE lighting simulation and rendering system,” in *Proceedings of 21st International SIGGRAPH Conference, 24-29 July 1994*, 1994, pp. 459–72.
[22] S. J. Emmerich and A. K. Persily, “U.S. Commercial Building Airtightness Requirements and Measurements,” in *AIVC Conference 2011*, Brussels, 2011.
[23] K. Gowri, D. W. Winiarski, and R. E. Jarnagin, “Infiltration modeling guidelines for commercial building energy analysis,” PNNL-18898, 968203, Sep. 2009.
[24] L. Guan, “The influence of internal load density on the energy and thermal performance of air-conditioned office buildings in the face of global warming,” *Archit. Sci. Rev.*, vol. 58, no. 2, pp. 162–173, Apr. 2015.
[25] A. Pandharipande and D. Caicedo, “Daylight integrated illumination control of LED systems based on enhanced presence sensing,” *Energy Build.*, vol. 43, no. 4, pp. 944–950, Apr. 2011.
[26] ISO Standard 7730, “Moderate thermal environments - Determination of the PMV and PPD indices and specification of the conditions for thermal comfort.” ISO, 1994.
[27] M. De Carli, B. W. Olesen, A. Zarrella, and R. Zecchin, “People’s clothing behaviour according to external weather and indoor environment,” *Build. Environ.*, vol. 42, no. 12, pp. 3965–3973, décembre 2007.
[28] Solar Energy Laboratory, University of Wisconsin-Madison, “TRNSYS 17 a TRaNsient SYstem Simulation program - Volume 5 - Multi zone Building modeling with Type56 and TRNBuild.” 2012.

[29] M.-C. Dubois and Å. Blomsterberg, “Energy saving potential and strategies for electric lighting in future North European, low energy office buildings: A literature review,” *Energy Build.*, vol. 43, no. 10, pp. 2572–2582, Oct. 2011.
[30] EnergyPlus™ Version 8.5 Documentation, “Engineering Reference.” U.S. Department of Energy, 31-Mar-2016.
[31] J. Wienold and J. Christoffersen, “Evaluation methods and development of a new glare prediction model for daylight environments with the use of CCD cameras,” *Energy Build.*, vol. 38, no. 7, pp. 743–757, juillet 2006.
[32] A. Nabil and J. Mardaljevic, “Useful daylight illuminance: a new paradigm for assessing daylight in buildings,” *Light. Res. Technol.*, vol. 37, no. 1, pp. 41–57, Mar. 2005.
[33] E. S. Lee *et al.*, “Advancement of Electrochromic Windows,” *Lawrence Berkeley Natl. Lab.*, Apr. 2006.
[34] M. N. Assimakopoulos, A. Tsangrassoulis, M. Santamouris, and G. Guarracino, “Comparing the energy performance of an electrochromic window under various control strategies,” *Build. Environ.*, vol. 42, no. 8, pp. 2829–2834, Aug. 2007.
[35] G. van Moeseke, I. Bruyère, and A. De Herde, “Impact of control rules on the efficiency of shading devices and free cooling for office buildings,” *Build. Environ.*, vol. 42, no. 2, pp. 784–793, Feb. 2007.
[36] S. Firląg *et al.*, “Control algorithms for dynamic windows for residential buildings,” *Energy Build.*, vol. 109, pp. 157–173, Dec. 2015.
[37] J.-M. Dussault, C. Kohler, H. Goudey, R. Hart, L. Gosselin, and S. E. Selkowitz, “Development and assessment of a low cost sensor for solar heat flux measurements in buildings,” *Sol. Energy*, vol. 122, pp. 795–803, Dec. 2015.
[38] A. Saltelli *et al.*, “2.4.4 Fractional Factorial Sampling,” in *Global sensitivity analysis*, John Wiley & Sons Ltd, 2008.
[39] J.-M. Dussault, L. Gosselin, and T. Galstian, “Integration of smart windows into building design for reduction of yearly overall energy consumption and peak loads,” vol. 86, no. 11, pp. 3405–16, Nov. 2012.
[40] E. Lee, “Energy and visual comfort performance of electrochromic windows with overhangs,” *Build. Environ.*, vol. 42, no. 6, pp. 2439–2449, 2007.
[41] A. Tavil and E. S. Lee, “Effects of Overhangs on the Performance of Electrochromic Windows,” *Archit. Sci. Rev.*, vol. 49, no. 4, pp. 349–356, Dec. 2006.
[42] E. S. Lee, S. Selkowitz, V. Bazjanac, V. George, and C. Kohler, “High-Performance Commercial Building Façades.” LBNL-50502, Lawrence Berkeley National Laboratory, Jun-2002.
[43] E. S. Lee, C. Gehbauer, B. E. Coffey, A. McNeil, M. Stadler, and C. Marnay, “Integrated control of dynamic facades and distributed energy resources for energy cost minimization in commercial buildings,” *Sol. Energy*, vol. 122, pp. 1384–1397, Dec. 2015.

5 Figure captions